2015 IEEE 54th Annual Conference on Decision and Control (CDC)
December 15-18, 2015. Osaka, Japan

Road Profile Classification for Vehicle Semi-active Suspension System Based on Adaptive Neuro-Fuzzy Inference System

Yechen Qin, Mingming Dong, Feng Zhao, Reza Langari, *Senior Member, IEEE*, and Liang Gu

***Abstract* — To meet the requirements of excitation information for semi-active suspension control, a new road classification method with application of Adaptive Neuro-Fuzzy Inference System (ANFIS) was presented. Due to distinct system responses for different road levels, the sprung mass acceleration signal was utilized for classification. To analyze the properties of various road inputs from different perspectives, the acceleration signal was first decomposed into 5 categories via wavelet transform, and 11 statistic features were calculated for each category. Then, an improved distance evaluation technique was applied to remove irrelevant features. With the extracted superior features, a new 2-layers ANFIS classifier was implemented to calculate overall road level. Simulation results revealed that the proposed classifier had significantly improved performance compared to all 1-layer ANFIS classifiers for individual category, and can accurately classify road level with negligible time delay.**

I. Introduction

Vehicle system responses directly depends on the characteristics of road profile, and road input has a significantly influences on the aspects related to vehicle safety (road handling), ride comfort, fuel consumption and forces/moments transmitted from the suspension system. Thus, precise estimation of road excitation is essential to improve vehicle performance of controllable suspension system.

Over the past decades, three road estimation and reproduction methods were widely used:

- *Direct measurement* employs specially designed profilometers to measure irregularity using mechanisms which are kept in contact with the road surface[1]. Although this method can provide precise profile measurements, structure of the profilometers restrict application in ordinary cars.
- *Road estimation based on vehicle response* use sensors, e.g. accelerometers, displacement sensors, and tilt angle sensor. These sensors collect response data and use sliding mode observer[2], transform function method[3, 4] or adaptive neural network[5] to estimate the road profile.
- *Non-contact measurement* utilizes vehicles equipped non-contact transceivers to measure the road profile[6]. However, the expense of transceivers restricts commercial application.

Since excitation from road unevenness is mostly filtered by suspension system, performance of suspension system thus has significant effects on vehicle response. To solve the essential conflict of ride comfort and road handling, the concept of controllable suspension system was introduced[7]. Based on energy consumption, controllable suspension systems can be further divided into active and semi-active[8].

To achieve superior performance, one possible selection is to combine road information with controllable suspension system. For active suspension system, road irregularity in time domain always act as feedforward signal[9] and be applied for optimal control or model predictive control (MPC)[10, 11]. Whereas, in the case of semi-active suspension, statistical information related to the road profile (e.g. road level) is typically applied to modified skyhook or hybrid control strategies[12]. However, even though the combination of road detection and control strategies have been proved more efficacious[9], most of the previously mentioned research reports assumed that the road is known in advance, and to the authors' best knowledge, little to no research has been reported in the literature related to precise acquisition of road information for a controllable suspension system.

A novel road level classification method for vehicle semi-active suspension system is proposed. Based on vehicle response, with the predefined control strategy, road input can be acquired and classified with the proposed algorithm. To better illustrate the mechanism of the algorithm, sprung mass acceleration generated from a nonlinear quarter vehicle model with skyhook control strategy was utilized. Sprung mass acceleration was decomposed into 5 categories in both time and frequency domains using wavelet transform and 11 statistical features for each category was then calculated. To avoid the curse of dimensionality, the improved distance evaluation technique[13] was applied to select the most relevant features. With the superior features, a 2-layers ANFIS classifier is used to finally estimate the road level.

There are three major advantages of the novel method discussed in this paper. First, the proposed classification approach is based solely on the vehicle's sprung mass acceleration signal, which allows easy implementation of this method. Second, since the basis of the method is the differences of the sampled signal in time and frequency domain, this allows wide range of application of this method to various control strategies with road excitation of varying frequency structure. Finally, this method differs from other

Reza Langari is with the Department of Mechanical Engineering, Texas A&M University, College Station, TX, 77840, USA. Email: rlangari@tamu.edu

All other authors are with School of Mechanical Engineering, Beijing Institute of Technology, Beijing, 100081, China. Corresponding author: Liang Gu, Phone: +86-68914005, E-mail: guliang@bit.edu.cn

978-1-4799-7886-1/15/$31.00 ©2015 IEEE

estimation methods as the proposed approach is model-free, which can take the suspension system characteristics that are hard to be depicted into consideration.

II. Road Profile Model

Often, road profile was assumed to be homogeneous and isotropic Gaussian processes and its characteristics can be described by Power Spectral Density (PSD). This paper established the road surface model according to ISO8601[14], and PSD of road roughness can be approximated by:

$$G_q(n) = G_q(n_0)\left(\frac{n}{n_0}\right)^{-W} \tag{1}$$

where n is the spatial frequency in m^{-1} and n_0 is the reference spatial frequency with a value of $0.1\mathrm{m}^{-1}$, $G_q(n_0)$ is the PSD for the reference frequency in m^3, W is called waviness, and it is assuming $W = 2$ in this paper.

For analysis, the method of filtered white noise was used to generate road irregularities, according to:

$$\dot{x}_\mathrm{r} = -2\pi f_0 x_\mathrm{r} + \sqrt{G_q(n_0)v}w \tag{2}$$

where $f_0 = 0.1\mathrm{Hz}$ is the low cut-off frequency and different road levels are classified by the value of $G_q(n_0)$.

III. Vehicle Model and Skyhook Control

Quarter vehicle model and skyhook control, which are the most commonly used model and control algorithms used for semi-active suspension systems, are discussed in this section.

A. Quarter Vehicle Model

The structure of a quarter vehicle model is shown in Fig.1, and Table I presents the parameters used for the model.

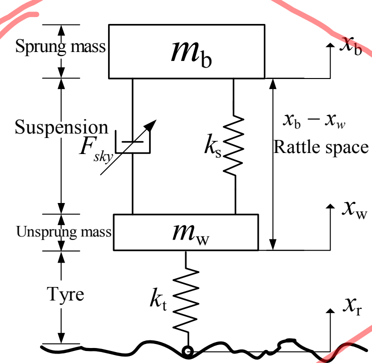

Figure 1. Model of quarter vehicle

Dynamic equations of the model are given by:

$$\begin{aligned} m_\mathrm{b}\ddot{x}_\mathrm{b} + F_{ks} + F_{sky} &= 0 \\ m_\mathrm{w}\ddot{x}_\mathrm{w} + k_\mathrm{t}\left(x_\mathrm{w} - x_\mathrm{r}\right) - F_{ks} - F_{sky} &= 0 \end{aligned} \tag{3}$$

where F_{ks} is the spring force, and the relationship between rattle space and spring force can be expressed as[15]:

$$F_{ks} = k_1 x_{rs} + \varepsilon k_1 x_{rs}^3 \tag{4}$$

where ε is the coefficient and k_1 stands for linear component. x_{rs} is the rattle space.

TABLE I. Quarter Vehicle Parameters

Parameters	Description	Values
m_b	Sprung mass	430 kg
m_w	Unsprung mass	46 kg
k_t	Tire stiffness	261300 N/m
$c_{\min}$	Minimum damping	600 Ns/m
c_{sky}	Skyhook damping	2500 Ns/m
k_1	Linear stiffness	22000 N/m
ε	Stiffness coefficient	3

B. Skyhook Control

Since firstly proposed in 1970s[16], skyhook control has been widely accepted as a reference semi-active suspension control strategy. In this paper, skyhook control was applied to illustrate the proposed classification method. To mimic the behaviour of ideal skyhook damping, the following control rules need to be satisfied:

$$F_{sky} = \begin{cases} c_{\mathrm{sky}}\left(\dot{x}_\mathrm{b}\right), & \mathit{if}\ \left(\dot{x}_\mathrm{b} - \dot{x}_\mathrm{w}\right)\cdot\dot{x}_\mathrm{b} \ge 0 \\ c_{\min}\left(\dot{x}_\mathrm{b} - \dot{x}_\mathrm{w}\right), & \mathit{if}\ \left(\dot{x}_\mathrm{b} - \dot{x}_\mathrm{w}\right)\cdot\dot{x}_\mathrm{b} < 0 \end{cases} \tag{5}$$

With the road definition, vehicle model and control strategy, the sprung mass acceleration in both time and frequency domains for ISO-B to ISO-G are shown in Fig.2 (road levels ISO-A and ISO-H are omitted, however, the responses are similar to other road levels).

From Fig.2, it can be seen that with the increment of road level, response increases nearly proportional. In this case, with the application of information derived from both domains, difference based classification becomes possible.

IV. Feature Extraction and Selection

In this section, the obtained sprung mass acceleration signal is firstly decomposed via level-3 wavelet transform. Totally five categories are then generated, including three approximation components A_1, A_2, A_3, first detail component D_1 and original signal in time domain. Three most superior features for each category are then selected from 11 features through the improved distance evaluation technique[13].

Wavelet Transform (WT) can be thought of as an extension of orthodox Fourier Transform (FT). To solve the problem emerge in the Short-Time Fourier Transform (STFT), WT decomposes signal into multiple-scales in both time and frequency domains. Each scale represents a certain component of the signal[17]. In this paper, after trial and error, the Daubechies wavelet of order 6 (db6) had the best performance and was selected as the wavelet basis function.

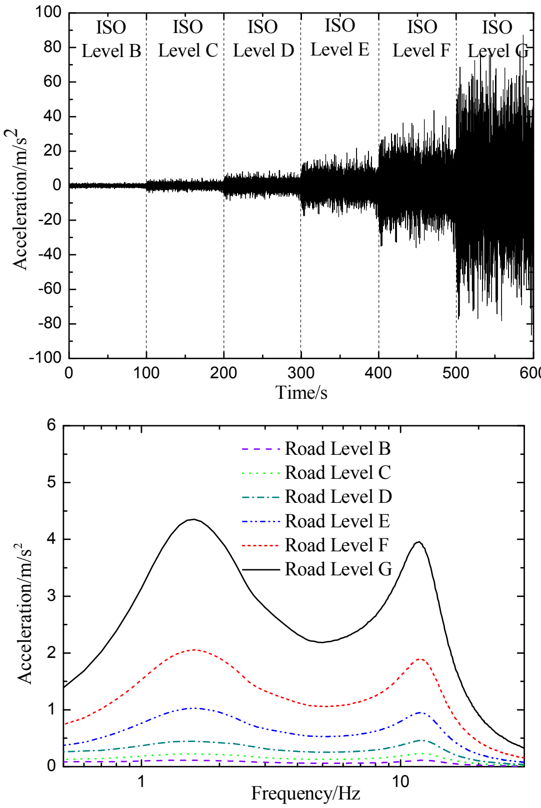

Figure 2. Acceleration response in time domain(up) and frequency domain(down)

To analyze characteristics of the 5 categories, a total of 11 features were used. The features are listed in Table II[18]. These parameters depict the investigated signal from different viewpoints. Parameters f_1 and $f_3 \sim f_5$ represent amplitude and energy, whereas parameters f_2 and f_{10} as along with $f_6 \sim f_7$ show distribution characteristics. Parameters $f_8 \sim f_9, f_{11}$ indicate influence of impact or impulse input.

Although all of 11 features listed in Table II can be applied to classify road excitation, each has different importance, i.e. sensitivity to diverse levels is different. In this case, a suitable method to select superior features is needed, and other unimportant features can be discarded to improve system performance, reducing training cost and avoid the problems associated with dimensionality. Here, improved distance evaluation technique, proposed by Lei[13, 18] was applied to choose the most relevant features. Procedure for the improved distance evaluation method is described in the following part.

Suppose a road feature set with C levels and J features can be described as:

$$\{q_{m,j,c}, m = 1,2,\cdots M, j = 1,2,\cdots J, c = 1,2,\cdots C,\} \quad (6)$$

where $q_{m,j,c}$ is the m^{th} sample of j^{th} feature belonging to the c^{th} level. M and J are the total number of samples and features, respectively. Distance evaluation procedure can be depicted in the following steps:

TABLE II. FEATURES DEFINITION

Parameters	Feature Name	Expression	Parameters	Feature Name	Expression
f_1	Mean value	$\frac{\sum_{n=1}^{N} x(n)}{N}$	f_7	Kurtosis	$\frac{\sum_{n=1}^{N}(x(n)-f_1)^4}{(N-1)f_2^4}$
f_2	Variance	$\sqrt{\frac{\sum_{n=1}^{N}(x(n)-f_1)^2}{N-1}}$	f_8	Crest factor	$\frac{f_5}{f_4}$
f_3	Square root of amplitude	$\left(\sum_{n=1}^{N}\sqrt{\lvert x(n)\rvert}/N\right)^2$	f_9	Clearance factor	$\frac{f_5}{f_3}$
f_4	Root mean square	$\sqrt{\frac{\sum_{n=1}^{N}(x(n))^2}{N}}$	f_{10}	Shape factor	$\frac{f_4}{\frac{1}{N}\sum_{n=1}^{N}\lvert x(n)\rvert}$
f_5	Maximum	$\max\lvert x(n)\rvert$	f_{11}	Impulse factor	$\frac{f_5}{\frac{1}{N}\sum_{n=1}^{N}\lvert x(n)\rvert}$
f_6	Skewness	$\frac{\sum_{n=1}^{N}(x(n)-f_1)^3}{(N-1)f_2^3}$			

- Step 1. Calculate average distance for samples at the same level.

$$d_{j,c}=\frac{2\times\sum_{k,l}^{M}\left|q_{k,j,c}-q_{l,j,c}\right|}{M\times\left(M-1\right)},k,l=1,2,\cdots M,k\neq l \quad (7)$$

Next, calculate average distance for the entire C level:

$$d_j^{(w)}=\sum_{c=1}^{C}d_{j,c}/C \quad (8)$$

- Step 2. Define and calculate the sample variance factor $v_j^{(w)}$

$$v_j^{(w)}=\frac{\max\left(d_{j,c}\right)}{\min\left(d_{j,c}\right)} \quad (9)$$

- Step 3. Calculate average value of samples at the same level

$$u_{j,c}=\sum_{m=1}^{M}q_{m,j,c}/M \quad (10)$$

Next, derive average distance between different levels:

$$d_j^{(b)}=\frac{2\times\sum_{p,q}^{C}\left|q_{j,p}-q_{j,q}\right|}{C\times\left(C-1\right)},p,q=1,2,\cdots C,p\neq q \quad (11)$$

- Step 4. Define and calculate level variance factor $v_j^{(b)}$

$$v_j^{(b)}=\frac{\max\left(\left|u_{j,p}-u_{j,q}\right|\right)}{\min\left(\left|u_{j,p}-u_{j,q}\right|\right)} \quad (12)$$

- Step 5. Calculate overall variance factor λ_j

$$\lambda_j=\frac{1}{\frac{v_j^{(w)}}{\max\left(v_j^{(w)}\right)}+\frac{v_j^{(b)}}{\max\left(v_j^{(b)}\right)}} \quad (13)$$

- Step 6. Calculate the overall distance factor α_j

$$\alpha_j=\lambda_j\cdot d_j^{(b)}/d_j^{(w)} \quad (14)$$

Next, normalize and obtain the final distance evaluation criterion $\bar{\alpha}_j$:

$$\bar{\alpha}_j=\frac{\alpha_j}{\max\left(\alpha_j\right)} \quad (15)$$

Features with higher $\bar{\alpha}_j$ can be thought to be more obvious than the others. Some features are then collected to form the superior feature set and can be further used in the formulation of the system classifier. Value of M,J,C and superior features set are defined as follows: $M=100$ for each level in the classifier training process, corresponding to the training and testing samples, $J=11$ stands for the 11 features listed in Table II, $C=8$ represents the standard 8 levels road excitation. In this paper, 3 features with largest distance evaluation criterion values were selected to compose the superior feature set.

V. FORMULATION OF ANFIS CLASSIFIER

After wavelet transform and distance evaluation processes, a superior feature set containing 3 features was obtained. It should be noted that for different categories, i.e. wavelet transform result from the same signal, components of the superior feature set might be diverse. In this case, all of the 5 categories in this paper are calculated separately according to the improved distance evaluation technique.

Adaptive Neuro-Fuzzy Inference System (ANFIS) was firstly proposed by Jang in 1993[19]. This method integrates back-propagation (BP) and the least squares estimation (LSE), realizing identification of structure and parameters of TS fuzzy system with neural network. A lot of successful applications have been reported, and in this paper, the ANFIS is acting as a classifier.

The classifier applied in this paper is a hybrid 2-layers ANFIS classifier. With the superior feature set, first layer ANFIS classifier was used to roughly separate road levels for the 5 categories signals. To further improve accuracy of classification, a combination of multiple classifiers technique was then utilized. The second layer ANFIS classifier takes five coarse outputs of the first layer ANFIS classifier as system input and generates the output, which is the overall classification result.

It should be further noted that for ANFIS training process, number and shape of Membership Function (MF) can be changed and both parameters will profoundly affect classification results. To the authors' best knowledge, no standard method is available to decide number and shape of MFs for ANFIS (with grid partitioning). As a result, after trial and error, in the simulation part, number of MFs for both ANFIS classifier is set as 4, and the shape is chosen as bell shape.

VI. SIMULATION

With road excitation and nonlinear quarter vehicle model defined in Section II and III, the 2-layers ANFIS classifier was first trained and a random road excitation of different levels was then generated to validate the proposed method.

With the assumption that the vehicle is traveling along the road with a velocity of 40km/h, a standard road profile with 8 standard levels was firstly generated. Each level has a total time period of 100 seconds. The vehicle mass acceleration response was generated with the application of skyhook control strategy. Acceleration signal for 800 seconds was applied to perform the feature selection and then, to train the 2-layers ANFIS classifiers. Response for the first 50 seconds for each road level was combined to generate the training set. The remaining 50 seconds response from each level were reshaped and treated as testing set to verify the accuracy and effectiveness of the generated ANFIS classifier's structure. Since for vehicle suspension system, the frequency range under consideration was always below 50Hz[5], the sample rate in this part was chosen as 100Hz. To avoid aliasing, a low-pass filter with cut-off frequency of 50Hz was applied.

With the calculated 5 categories, feature selection was carried out for each category. Fig.3 shows results of the selection, and it can be seen for all of these five categories that features 3,4 and 5, i.e. the square root of amplitude, root mean square and maximum, respectively, have the highest relative distance value. This means that these three features can best present diversity for different road levels compared with other 8 features. Recall features definitions from Section IV, since there is no impact input or distribution variation during the generation of road profile, it can explain the reason for small distance values of all other features.

To better illustrate disparity of 8 road levels and to demonstrate accuracy of feature selection, 11 features of category 1 are shown in Fig.4. It can be clearly seen that features 3,4, and 5 show obvious gap for all 8 road levels, whereas other features cannot be used to classify the road level.

After feature selection is performed, the superior feature set was applied to train 2-layers ANFIS classifier. To show the necessity of the proposed 2-layers ANFIS classifier, a comparison between 1-layer ANFIS for all 5 categories and 2-layers ANFIS (hybrid) is presented. Classification accuracy and corresponding RMSE (Root mean square error) are tabulated in Table III. It should be noticed that for the output road level y, classification accuracy is defined by checking whether it belongs to set A (assuming the correct output is y^*)

$$A = \left\{ y \in \Re^+ \mid y^* - 0.5 \le y \le y^* + 0.5, y^* = 1, 2, \cdots 8 \right\} \quad (16)$$

Based on Table III, the proposed 2-layers ANFIS classifier was observed to be significantly better than all 1-layer ANFIS classifiers. Compared with the best 1-layer ANFIS classifier, overall accuracy was raised from 93.1% to 100%, training error decreased from 0.133 to 0.005, and testing error reduced from 0.211 to 0.091.

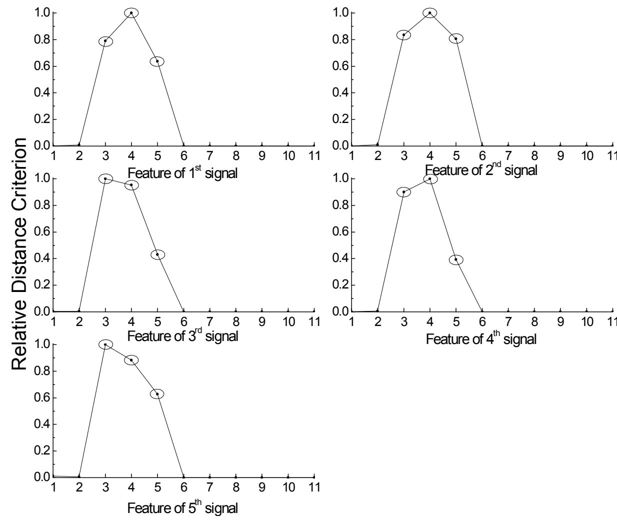

Figure 3. Superior feature selection of 5 signals

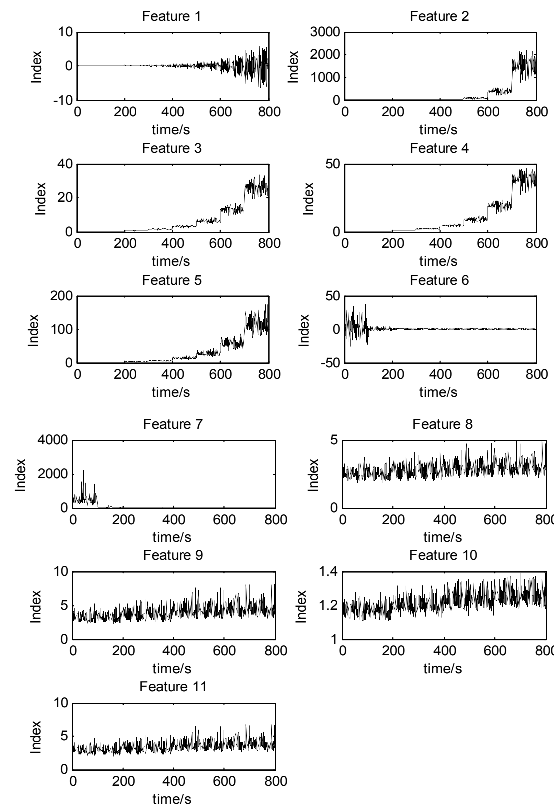

Figure 4. 11 features of category 1

TABLE III. COMPARISON OF 1-LAYER AND 2-LAYERS ANFIS CLASSIFIER

Results		1-layer Category 1	1-layer Category 2	1-layer Category 3	1-layer Category 4	1-layer Category 5	2-layers Hybrid
Overall Accuracy	Training	100%	100%	96.8%	89.3%	96.2%	100%
	Testing	90.6%	93.1%	94.3%	79.3%	95%	100%
RMSE	Training	0.121	0.133	0.219	0.274	0.201	0.005
	Testing	0.231	0.211	0.208	0.601	0.212	0.091

To validate the proposed method, new road was generated. The new profile is composed of five road levels: levels B, D, E, F and C, in successive order. The classification interval is set be 1 second and the result with 2-layers ANFIS classifier for the new road profile is represented in Fig.5.

As seen in Fig.5, some local errors appear during the classification process, however, overall output levels still belong to set A. This implies that the classification accuracy of this new-generated road is 100%. It can also be seen that the classified road levels converge quite rapidly to fit new road levels, which means that although the levels gap is large (from level F to level C), delay in the classification procedure was negligible for classification interval of 1 second.

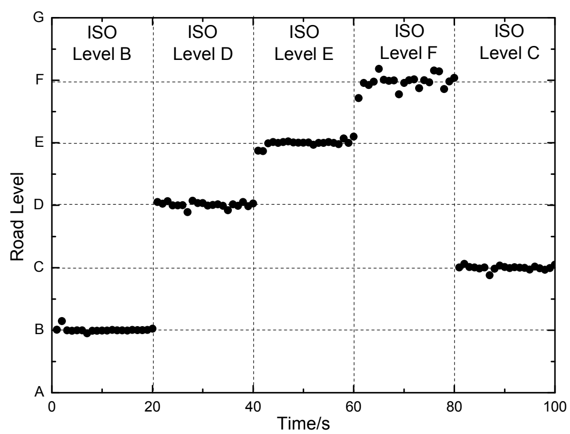

Figure 5. Classification results for the newly generated road profile

VII. CONCLUSION

In this paper, a new road profile classification method for semi-active suspension system based on wavelet transform, improved distance evaluation, and ANFIS was presented. To improve effectiveness of the method, skyhook control strategy was applied to a quarter vehicle model, and sprung mass acceleration signal was utilized for classification. The obtained sprung mass acceleration signal was first decomposed by wavelet transform, and 11 different statistical features were derived for 5 categories. To remove irrelevant features, an improved distance evaluation technique was applied to select superior feature sets. With these categories and a superior feature set, a 2-layers ANFIS classifier was utilized to classify road level input. Simulation results reveal that the proposed method can accurately and rapidly classify different road levels, and shows a much higher accuracy compared to single ANFIS classifier for individual category. Result indicates that this method can be applied for road detection in semi-active suspension system in future studies.

The road input used in this paper was the 8 levels ISO road profile. From practical application perspective, actual roads may different from the specified ISO road, especially in terms of waviness W and the reference PSD value $G_q(n_0)$. Each of these would, lead to different response. In this case, the proposed method was still applicable since it was completely dependent on the differences of system responses in both time and frequency domain. Since the proposed method was based only on theoretical analysis and validation using simulations, an actual bench test for a quarter vehicle model is being developed and results from the experiment will be reported in the near future.

REFERENCE

[1] M.Doumiati, A. Victorino and A. Charara. "Estimation of road profile for vehicle dynamics motion: experimental validation". *Proc. of American Control Conference*. San Francisco, CA, June 29-July 1, 2011.

[2] A. Rabhi, N.K. M'sirdi and L. Fridman. "Second order sliding mode observer for estimation of road profile". *Proc. of the 2006 International workshop on Variable Structure Systems*. Italy.

[3] A.Gonzalza, E.J.O'brien and K.Cashell. "The use of Vehicle Acceleration Measurements to Estimate Road Roughness". *Vehicle System Dynamics*, vol. 46, no. 6, pp. 483-499, June 2008.

[4] Y.C. Qin, J.F. Guan and L. Gu. "the Research of Road Profile Estimation Based on Acceleration Measurement". *Applied Mechanics and Materials*, vol. 226-228, pp. 1614-1617, July 2012.

[5] Y.C. Qin, R. Langari and L. Gu. "The use of vehicle dynamic response to estimate road profile input in time domain". *Proc. of ASME DSCC*. San Antonio, TX, Dec. 15-18, 2014.

[6] R. Mccann and S. Nguyen. "System identification for a model-based observer of a road roughness profiler". *2007 IEEE Region 5 Technical Conference*. Fayetteville, AR, Apr. 20-21, 2007.

[7] S.M. Savasel, C.P. Vassal and C. Spelta. *Semi-active suspension control design for vehicles*. MA: Elsevier, 2010. pp. 14-20.

[8] D.Hrovat. "Survey of advanced suspension developments and related optimal control applications". *Automatica*, vol. 33, no. 10,pp. 1781-1817, Oct 1997.

[9] A. Hac and I. Youn. "Optimal design of active and semi-active suspensions including time delays and preview". *Transactions of the ASME*, vol. 115, pp. 498-508, July 1993.

[10] M. Elmadary, A.B. Bassam and A. Fayed. "Preview control of slow-active suspension systems". *Journal of Vibration and Control*, No. 1077546310362451, Oct 2010.

[11] C. Gohrle, A. Schindler and A. Wagner. "Design and Vehicle Implementation of Preview Active Suspension Controllers". *IEEE Transactions on Control Systems Technology*, vol. 22, no. 3, pp. 1135-1152, Mar 2014.

[12] K.S. Hong, H.C. Sohn and J.K. Hedrick. "Modified skyhook control of semi-active suspensions: A new model, gain scheduling, and hardware-in-the-loop tuning". *Journal of Dynamic Systems, Measurement, and Control*, vol. 124, no. 1, pp. 158-167, Jan 2002.

[13] Y.G. Lei, Z.J. He and Y.Zi. "A new approach to intelligent fault diagnosis of rotating machinery". *Expert systems with applications*, vol. 35, pp. 1593-1600, Sep 2008.

[14] ISO. *Mechanical Vibration-Road Surface Profiles-Reporting of measured data*. ISO8601-1995, 1995.

[15] M. Mitschke and H. Wallentowitz. *Vehicle dynamics*. Beijing: TsingHua Press, 2010, in Chinese. pp. 456-490.

[16] D. Karnopp, M.J. Crosby and R. Harwood. "Vibration control using semi-active force generators". *Journal of Engineering for Industry*, vol. 96, no. 2, pp. 619-626, Feb 1974.

[17] S.G. Mallat. "A theory for multiresolution signal decomposition: the wavelet representation". *IEEE Transactions on Pattern Analysis and Machine Intelligence*, vol. 11, no. 7, pp. 674-693, Nov 1989.

[18] Y.G. Lei, Z.J. He, Y.Y. Zi. "Fault diagnosis of rotating machinery based on multiple ANFIS combination with GAs". *Mechanical systems and signal processing*, vol. 21, pp. 2280-2294, Mar 2007.

[19] J.S.R. Yang. ANFIS: "Adaptive-Network-Based Fuzzy Inference System". *IEEE Transactions on systems, man, and cybernetics*, vol. 23, no. 3, pp. 665-685, Mar 1993.